EVOJES
EcoVision: Journal of Environmental Solutions
EVOJES 3(1): 87-108
ISSN 3046-8434

Institute for Advanced Science, Social and Sustainable Future
MORALITY BEFORE KNOWLEDGE

Future drought characteristics in Sumatra under shared socioeconomic pathways 5-8.5 based on the standardized precipitation index

Asshaffa Naim[1,*]
[1] *Department of Environmental Geography, Faculty of Geography, Universitas Gadjah Mada, Sleman, Special Region of Yogyakarta 55281, Indonesia.*
*Correspondence: asshaffa.naim@mail.ugm.ac.id

Received Date: November 12, 2025 Revised Date: January 25, 2026 Accepted Date: February 28, 2026

ABSTRACT
Background: Climate change has increased the intensity and frequency of droughts globally and affected freshwater availability, particularly in developing regions with limited adaptive capacity. In Sumatra, prolonged droughts and reduced rainfall have increased vulnerability to drought, necessitating accurate projections to support climate resilience and sustainable water management. This study aims to assess drought projections in Sumatra from 2015 to 2100 in the Shared Socioeconomic Pathways 5-8.5 (SSP 5-8.5), which represents a high emission trajectory. **Methods**: CMIP6 monthly precipitation from the CMIP6 EC-Earth3 model was bias-corrected using Monthly Mean Bias Correction. The corrected precipitation was used to calculate Standardized Precipitation Index (SPI) to evaluate future drought conditions based on rainfall distribution. **Findings:** The SPI calculation results show that the frequency of severe droughts (SPI < -1.5) experiences significant interannual fluctuations, in line with rainfall patterns that exhibit oscillatory patterns every few years. The southern part of Sumatra emerged as the most drought-prone region with more than 140 drought events detected. The highest drought vulnerability occurs between March and May in the northern region, which has an equatorial rainfall pattern, while the peak drought vulnerability occurs between September and November in the southern region. Atmospheric circulations such as the ITCZ, ENSO, and IOD, as well as topographic and geographic factors, play a crucial role in regulating drought in Sumatra. **Conclusion**: Future droughts in Sumatra will be more frequent, occurring in short but severe periods compared to weak, long-lasting droughts. The influence of atmospheric circulation will change with climate change and future anthropogenic pressures, increasing the unpredictability of droughts. **Novelty/Originality of this article:** This study integrates climate projections with robust and efficient drought index calculations to assess future droughts. Supported by comprehensive spatio-temporal analysis, the findings of this study can provide key-insights for climate resilience and sustainable meteorological-based water management efforts. However, uncertainties remain related to single-model dependency, emission scenario assumptions, and SPI's precipitation-only formulation.

KEYWORDS: climate projection; drought; standarized precipitation index; Sumatra.

1. Introduction

Climate change has been a crucial environmental issue for the last century and will continue to be a global focus in the future. The global climate system has experienced an increase in atmospheric temperature of approximately 1.1°C above pre-industrial levels due to the accumulation of greenhouse gases from human activities (IPCC, 2023). This temperature increase has triggered intensification in the frequency and magnitude of

Cite This Article:
Naim, A. (2026). Future drought characteristics in Sumatra under shared socioeconomic pathways 5-8.5 based on the standardized precipitation index. *EcoVision: Journal of Environmental Solutions, 3*(1), 87-108. https://doi.org/10.61511/evojes.v3i1.2026.3123

climate-related extremes such as heatwaves, floods, and, most noticeably, droughts (Tuel et al., 2021; Batibeniz et al., 2023; Singh et al., 2023). Globally, over four billion people experiencing water scarcity each year due to drought, and it is projected to raise as climate change accelerates (Mukasa et al., 2020; He et al., 2021). Drought-induced water scarcity caused by the reduction of rainfall and depletion of groundwater reserves is disrupting agricultural productivity, compromising hydropower generation, and limiting access to clean water for domestic and industrial use (Mahadevan et al., 2024). These effects burden developing countries where water infrastructure and management systems are often insufficient.

As one of the largest and most populous islands in Indonesia, Sumatra serves as a vital center for agriculture, forestry, and energy production. However, the island's hydrological systems are increasingly vulnerable to climate-induced perturbations. Prolonged dry seasons, declining rainfall in critical months, and intensified land-use changes have placed substantial pressure on freshwater resources (Irwandi et al., 2021). The combination of natural climatic variability and anthropogenic land transformation has led to periodic water scarcity crises that affects both rural livelihoods and urban water supplies. As climate change progresses, these challenges are expected to intensify, making Sumatra a priority region for drought projection and adaptive water management research.

The rising frequency and intensity of drought events highlight the need for reliable and standardized tools to measure and monitor drought conditions. Standardized Precipitation Index (SPI) has emerged as one of the most widely used and internationally recognized indicators. Developed by McKee et al. (1993), the SPI is based solely on precipitation data, making it computationally straightforward and adaptable to regions with limited climate records. Numerous studies have demonstrated the effectiveness of SPI in various global and regional contexts. Research by Zeng et al. (2022) found that SPI is particularly effective in regions with robust drying trends such as the southwestern United States, Amazon Basin, Mediterranean, southern Africa, southern Asia, and Australia. In Yellow River Basin, China, SPI has been used to explore spatial heterogeneity in drought conditions, with precipitation identified as the predominant driver (Gao et al., 2024). Across Asia, SPI has been applied in countries such as India, Malaysia, and China to analyze drought dynamics and their relationship with climatic drivers like ENSO and IOD (Johny et al., 2020; Wang et al., 2022; Suhana et al., 2023).

In Indonesia, SPI is operationally adopted by the Meteorology, Climatology, and Geophysics Agency (BMKG) for real-time drought monitoring and early-warning dissemination. SPI can be calculated over different timescales (e.g. 3, 6, 12 months), therefore allowing it to capture short-term agricultural droughts as well as long-term hydrological droughts (Zhang & Li, 2020). Its success in reflecting regional rainfall variability and correlation with agricultural yield losses underscores its applicability for tropical environments. SPI is therefore adopted as an effective indicator for characterizing meteorological drought and examining precipitation-driven variability under future climate scenarios. Combined with bias-corrected precipitation data from CMIP6 climate simulations, SPI enables a comprehensive and spatially explicit understanding of future drought risks under changing climatic conditions.

In scientific projections, the Shared Socioeconomic Pathway (SSP) 5–8.5 scenario assumes rapid economic growth driven by intensive energy use and continued reliance on fossil fuels, resulting in the highest projected global temperature increase among the SSP scenarios (O'Neill et al., 2017). This study adopts the SSP5–8.5 as an analytical framework for understanding the potential severity of future drought conditions, particularly in tropical developing regions like Indonesia, where adaptive capacity remains limited and climate exposure is high (Hendrawan et al., 2024). These future scenarios are physically simulated using Global Climate Models participating in the Coupled Model Intercomparison Project Phase 6 (CMIP6), which provides the latest generation of climate projections. Recent studies utilizing CMIP6 projections have demonstrated improved capability in representing future hydroclimatic conditions, particularly in simulating precipitation variability and temperature-driven moisture changes that are critical to drought formation (Ukkola et al., 2020). Under high-emission scenarios such as SSP5–8.5, many tropical regions are projected to experience increases in drought frequency, intensity, and duration, alongside shifts in spatial distribution of drought-prone areas driven by changes in regional circulation and land–atmosphere interactions (Ernst et al., 2025).

Over the past decade, research on drought in tropical regions has expanded significantly, with Sumatra emerging as a critical area of study due to its vulnerability to climate variability. The SPI and Effective Drought Index (EDI) shows that extreme droughts in Sumatera is heavily influenced by El Niño and positive IOD phenomena (Suhadi et al., 2023). The Consecutive Dry Days (CDD) metric further provides insight into dry-spell persistence, showing an increase of approximately 1.23 days per decade on Sumatra's eastern coast (Akhsan et al., 2023). Despite significant progress in drought assessment, the scientific understanding of future drought dynamics remains limited. Most existing studies have focused on historical or short-term analyses using observational or satellite-derived datasets that offers valuable retrospective insights but limited predictive power. Furthermore, past studies often analyzed droughts across broad regions without integrating the spatial variation of drought with its multi-temporal persistence. Therefore, there is an urgent necessity for research that bridges these limitations to anticipate future drought conditions with greater precision.

To address this problem and close the identified knowledge gaps, this research pursues the following overarching objectives. First, it aims to project the spatiotemporal characteristics of drought across Sumatra from 2015 to 2100 using bias-corrected CMIP6 precipitation data. Second, it seeks to identify drought-prone regions through spatial mapping and seasonal analysis to pinpoint areas most susceptible to intensified water deficits. Third, it endeavors to analyze the long-term trends and evolving patterns of drought to reveal how frequency, duration, and severity may shift under continued warming. Ultimately, this study aspires to produce a comprehensive scientific projection of drought in Sumatra under future climate scenarios and generating insights that are critical for adaptation planning, water resource management, and sustainable development.

2. Methods

This study focuses on Sumatra Island, located between 93°E–108°E and 8°S–8°N, covering an area of approximately 473,000 km^2 (Fig.1). Sumatra is one of the largest and most climatically diverse islands in Indonesia (Mareta et al., 2024). The island stretches longitudinally from Aceh in the north to Lampung in the south, bordered by the Indian Ocean on the west and the Malacca Strait on the east. Its topography is dominated by the Barisan Mountains, a volcanic range that forms a steep western corridor and creates a pronounced west–east rainfall gradient. Annual precipitation ranges from over 3,000 mm on the western slopes to less than 2,000 mm in the eastern lowlands, where droughts tend to be more persistent (Fathiyana et al., 2025). The climate is classified as humid tropical (Af–Am) with two primary seasons governed by the monsoon system: a wet season from November to April and a dry season from June to October (Liu et al., 2020). Interannual rainfall variability is strongly influenced by large-scale ocean–atmosphere phenomena, particularly the El Niño–Southern Oscillation (ENSO) and the Indian Ocean Dipole (IOD), both of which can suppress convection and delay the onset of the monsoon, triggering extended dry spells (Hadiningrum et al., 2023).

Observational and modeled climate datasets are utilized to assess and project drought conditions across Sumatra for the period 2015–2100. The datasets comprise (1) daily rainfall observations from selected BMKG (Meteorology, Climatology, and Geophysics Agency) stations, and (2) monthly precipitation outputs from the Coupled Model Intercomparison Project Phase 6 (CMIP6), specifically the EC-Earth3 model. The observational rainfall data were collected from 17 BMKG stations distributed across the island of Sumatra, representing various climatic and topographic conditions from coastal to inland regions. The selected stations were chosen based on spatial coverage, data continuity, and record completeness during the 2011–2014 baseline period. The observational data serve as the empirical reference for evaluating and correcting the bias of the CMIP6 precipitation data.

Fig. 1. Study Area

To ensure that the observational dataset adequately represents the spatial variability of rainfall across Sumatra, the selected BMKG stations encompass a wide range of geographic locations and elevation gradients. This spatial coverage is particularly important because the island exhibits substantial climatic heterogeneity resulting from complex topography, coastal–inland contrasts, monsoonal circulation, and the influence of large-scale climate phenomena such as the El Niño–Southern Oscillation (ENSO) and the Indian Ocean Dipole (IOD). Consequently, rainfall characteristics vary considerably between western coastal regions, mountainous areas along the Barisan Range, and eastern lowlands, making representative station selection essential for reliable climate analysis.

The use of observation stations distributed across different hydroclimatic zones also minimizes spatial sampling bias and improves the representativeness of the reference dataset used for model evaluation. Since climate models often exhibit systematic errors that vary geographically, observational data collected under diverse environmental conditions provide a stronger basis for identifying and correcting regional biases in simulated precipitation. This is particularly important for drought assessments, where relatively small errors in rainfall estimation may substantially influence drought severity classifications and future projections.

Furthermore, the selection of stations with continuous and relatively complete observation records enhances the consistency of the bias-correction procedure and reduces uncertainties associated with missing data. The combination of broad spatial coverage, varying elevations, and reliable observational records enables the dataset to capture both regional and local rainfall variability across Sumatra. Consequently, the BMKG observation network provides a robust empirical benchmark for evaluating the performance of the

CMIP6 EC-Earth3 model before its precipitation outputs are applied to future drought projections. The geographical distribution and characteristics of the BMKG observation stations used in this study are presented in Table 1.

Table 1. BMKG Observation Station

BMKG Stations	Longitude (°E)	Latitude (°N)	Elevation (mdpl)
Station Aceh	95.46	5.40	40
Station Cut Nyak Dhien Nagan Raya	96.25	4.05	3
Station Maimun Saleh	95.34	5.88	126
Station Deli Serdang	98.56	3.50	86
Station Aek Godang	99.45	1.55	281
Station Binaka	97.70	1.16	2
Station FL Tobing	98.88	1.55	10
Station Kualanamu	98.88	3.65	23
Station Maritim Teluk Bayur	100.37	-1.00	2
Station Sultan Mahmud Baddarudin II	104.70	-2.89	10
Station Sultan Syarif Kasim	101.45	0.46	39
Station Kepahiang	102.59	-3.55	517
Station Bengkulu	102.31	-3.87	12
Station Depati Parbo	101.45	-2.08	782
Station Sultan Thaha	103.64	-1.63	25
Station Maritim Panjang	105.32	-5.47	3
Station Radin Inten II	105.11	-5.16	94

As shown in Table 1, the observation stations are distributed across the major provinces of Sumatra, covering a broad range of longitudes, latitudes, and elevations from approximately 2 to 782 meters above sea level. This spatial diversity enables the dataset to capture variations in precipitation associated with topographic influences, coastal–inland gradients, and regional atmospheric circulation patterns that characterize the island. The inclusion of stations located in both lowland coastal areas and elevated inland regions improves the representativeness of the observational dataset for regional-scale drought assessment.

The comprehensive station network also provides a reliable basis for validating and bias-correcting the CMIP6 EC-Earth3 precipitation simulations. By comparing modeled precipitation with observations collected under diverse environmental conditions, the bias-correction procedure can better account for regional climatic variability and reduce systematic model errors. Consequently, the corrected climate projections provide a more robust foundation for the subsequent drought analyses and future climate projections presented in the following sections.

For future projection, this study employs monthly precipitation data from the CMIP6 EC-Earth3 model published by the Copernicus Climate Change Service (2021) with an approximate horizontal resolution of 1° × 1° (~100 km). Although this resolution may not fully represent localized rainfall variability, it is adequate for regional-scale analysis aimed at identifying broader drought patterns under future climate scenarios. The performance of CMIP6 models in simulating extreme precipitation indices indicated that EC-Earth3 was among the few models that successfully reproduced both spatial patterns and inter-annual variability (Tang et al., 2021). Meanwhile, study by Kurniadi et al. (2022) found that the EC-Earth3 model was highlighted for its consistent performance in simulating extreme precipitation indices in the region. The model data includes both the historical period (2011–2014) and the future projection (2015–2100) under the SSP5–8.5 scenario. A single-model approach was adopted to focus the analysis on the high-emission SSP5–8.5 trajectory as a plausible worst-case scenario, thereby emphasizing the characterization of potential drought responses under sustained warming rather than comparing differences among multiple model outputs or alternative scenarios.

This study adopts a quantitative and spatially explicit approach to analyze and project drought conditions across Sumatra for the period 2015–2100. The methodology integrates observational rainfall data with climate model simulations by applying statistical bias correction and drought index computation to quantify the temporal and spatial variability of drought events. Observational rainfall data from BMKG stations were spatially interpolated to create a continuous rainfall surface that could be directly compared with gridded climate model outputs. The interpolation was performed using the Inverse Distance Weighting (IDW) method to estimates values at unsampled locations. This interpolation method produce a spatially continuous gridded rainfall dataset based on the distance-weighted average of nearby observations to match the CMIP6 data structure (Fattorini et al., 2023). IDW is chosen because it is proven to be more reliable and efficient compared to another method like kriging and spline, particularly in interpolating precipitation (Daliakopoulos, 2021). This gridded observational dataset serves as the empirical baseline for model bias correction, ensuring that subsequent analyses are grounded in actual local rainfall conditions.

Climate models such as CMIP6 often exhibit systematic biases which can result in overestimation or underestimation of rainfall magnitude and variability (Liu et al., 2023). Therefore, bias correction is performed using Monthly Mean Bias Correction (MMBC) method so that the model data can better reflect local climatic conditions. This technique adjusts each monthly rainfall value of the model based on the ratio of observed to modeled means during the historical overlap period (Jo & Pak, 2022). Once the correction coefficients are determined, they are applied to the projected model data for the entire period (2015–2100). The correction factor is computed for each month using Eq. 1.

$$C_m = \frac{\overline{P_{obs,m}}}{\overline{P_{mod,m}}} \qquad \text{(Eq. 1)}$$

where C_m is the correction coefficient for month m, $\overline{P_{obs,m}}$ is the observed mean precipitation for month m (from BMKG interpolated data), and $\overline{P_{\mathrm{mod},m}}$ is the corresponding modeled mean from CMIP6 EC-Earth3 for the same period. Once the correction coefficients (C_m) are determined, they are applied to the projected model data for the entire period (2015-2100) using Eq.2.

$$P'_{mod,m,t} = P_{mod,m,t} \times C_m \qquad \text{(Eq. 2)}$$

where $P'_{\mathrm{mod},m,t}$ is the bias-corrected precipitation for month m at time t, and $P_{\mathrm{mod},m,t}$ is the original model output. Although this multiplicative bias-correction approach does not explicitly adjust higher-order variability or extremes, it effectively reduces systematic deviations in CMIP6 precipitation relative to observed rainfall and ensures that the monthly mean of the corrected model aligns with the observed climatology while preserving interannual variability.

The reliability of the bias correction was evaluated by comparing model outputs before and after correction using Root Mean Square Error (RMSE) and Pearson's correlation coefficient (r). Validation step ensured that bias-corrected model data accurately represented the magnitude and variability of observed rainfall, thereby providing a robust foundation for subsequent SPI analysis and drought projection. The corrected precipitation data were then aggregated as annual total precipitation and visualized using bar charts to provide a preliminary insight into projected rainfall behavior.

The results of the precipitation projection model data correction are used to calculate the SPI value. In this study, the 3-month SPI (SPI-3) was selected to represent short-term to seasonal drought conditions because of its ability to capture short-term variability, its applicability across different climates, and its practical utility in early warning systems and drought management (Cammalleri et al., 2024). The SPI was calculated for each grid point across Sumatra using monthly bias-corrected precipitation data from 2015 to 2100. The computation of SPI involves three main steps. First, the precipitation series for each grid cell and each 3-month accumulation period was fitted to a Gamma distribution, as precipitation values are positively skewed and bounded at zero. The probability density function (PDF) of the Gamma distribution is defined as Eq. 3.

$$f(x) = \frac{1}{\beta^{\alpha}\Gamma(\alpha)} x^{\alpha-1} e^{-\frac{x}{\beta}}, x > 0 \qquad \text{(Eq. 3)}$$

where α is the shape parameter, β is the scale parameter, and $\Gamma(\alpha)$ is the gamma function. Parameters α and β were estimated using the maximum likelihood method. Next, the cumulative probability $G(x)$ is computed as Eq. 4.

$$G(x) = \int_0^x f(t)dt \qquad \text{(Eq. 4)}$$

Because precipitation data often contain zero values, an adjusted cumulative probability $H(x)$ is derived as Eq. 5.

$$H(x) = q + (1 - q)G(x) \qquad \text{(Eq. 5)}$$

where q is the probability of zero precipitation. Finally, the cumulative probability $H(x)$ is transformed into a standard normal variable Z (with mean 0 and standard deviation 1), which represents the SPI value in Eq. 6.

$$\text{SPI} = \Phi^{-1}[H(x)] \qquad \text{(Eq. 6)}$$

where $\mathbf{\Phi}^{-1}$ is the inverse standard normal function. Negative SPI values indicate below-average rainfall (drought conditions), while positive values indicate wetter-than-normal conditions. Drought occurrence was identified when SPI-3 values fell below −1.5, which represents severe to extreme drought conditions. The frequency of such events was computed on an annual basis for each grid cell to quantify temporal patterns of drought incidence.

To reveal long-term temporal variability, the mean annual SPI and frequency of drought events (SPI < −1.5) were calculated for each year from 2015 to 2100. These time series were analyzed to characterize decadal-scale variability and the evolution of drought intensity and recurrence under the SSP5–8.5 scenario. Temporal patterns were visualized using line and bar charts to ilustrate fluctuations in drought occurrence across decades. Spatially, drought frequencies were mapped to identify regions that are most vulnerable to recurrent drought. Additionally, seasonal analyses were conducted for four climatological periods that consist of DJF (December–February), MAM (March–May), JJA (June–August), and SON (September–November) to assess how monsoonal transitions influence drought distribution. All computations were conducted using Python 3.11, with the xarray, numpy, and scipy.stats libraries for data handling and statistical operations. Visualization and spatial mapping were performed using matplotlib and cartopy. The integration of temporal and spatial analyses allows for a comprehensive understanding of how drought dynamics evolve both in time and across regions.

3. Results and Discussion

3.1 Data correction

Bias correction is a crucial step in climate model evaluation and projection because raw outputs often contain systematic errors that arise from model parameterizations, coarse spatial resolution, and imperfect representation of physical processes such as convection and orographic rainfall. Before using the CMIP6 precipitation data for drought analysis, a Monthly Mean Bias Correction (MMBC) was applied to adjust simulated rainfall toward the observed climatology derived from BMKG stations across Sumatra for the baseline period 2011–2014.

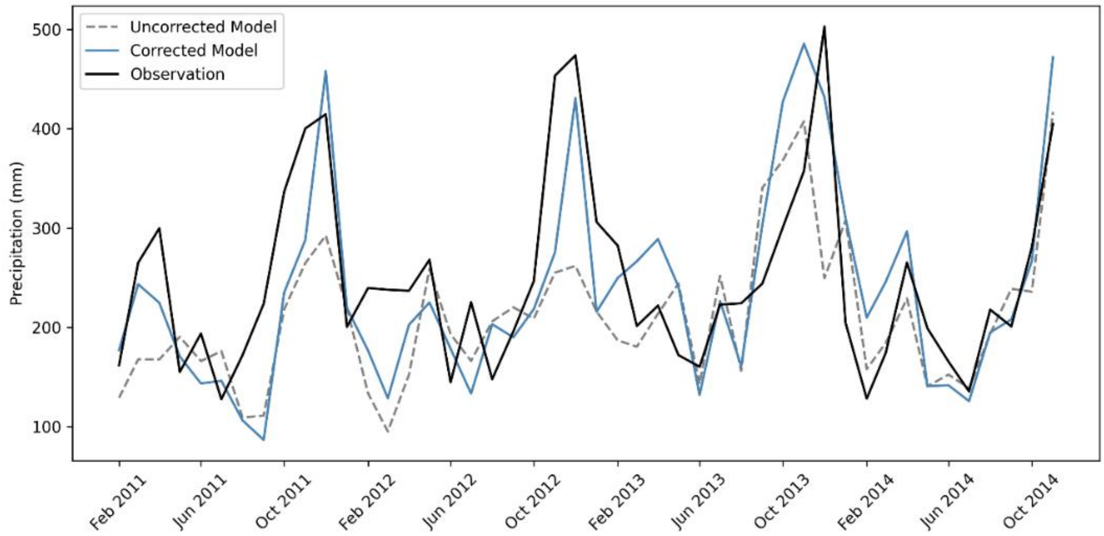

Fig. 2. Comparison of Uncorrected and Corrected Precipitation Model with Observation Data

The uncorrected EC-Earth3 precipitation data exhibited noticeable discrepancies compared to observed rainfall, particularly in regions with strong topographic control over precipitation such as the western Barisan Mountains and coastal lowlands (Fig. 2). The model tended to underestimate rainfall during the wet season (DJF–MAM) and overestimate it during the dry season (JJA–SON). This indicates a misrepresentation of the monsoon's amplitude and seasonal timing which are common in global climate models, especially where convective processes and complex land–sea interactions are difficult to simulate at coarse grid scales (Li et al., 2020; Kurniadi et al., 2022). After applying the correction, the model demonstrates a substantial improvement in following the observed rainfall pattern. The seasonal cycle becomes more consistent with observed conditions.

Fig. 3 presents the scatter relationship between observed precipitation (y-axis) and bias-corrected CMIP6 precipitation (x-axis) for all monthly data points between 2011 and 2014. The distribution of points reveals a strong positive correlation, where most values cluster along a near-linear trend, indicating a consistent increase in observed rainfall with increasing model rainfall. This pattern suggests that the bias correction process has significantly improved the linear relationship between the two datasets.

To further evaluate the effectiveness of the bias correction procedure, a statistical comparison between the corrected CMIP6 precipitation data and the observed rainfall records was performed. In addition to examining the spatial and seasonal rainfall patterns, the agreement between the two datasets was assessed through a scatter plot analysis. This approach enables the visualization of the relationship between corrected model outputs and observations, providing an indication of how well the bias-corrected dataset reproduces the magnitude and variability of observed precipitation.

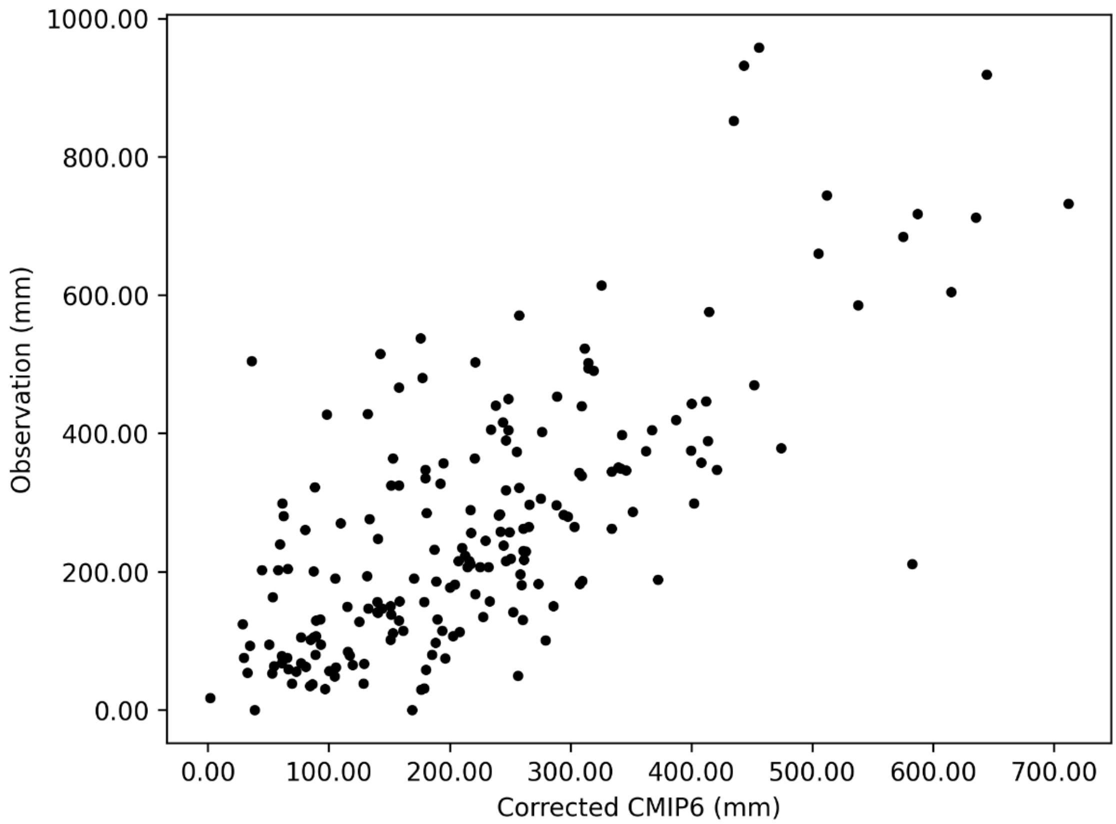

Fig. 3. Corrected CMIP6 vs Observation Precipitation Data Scatter Plot

Quantitatively, the correlation coefficient (r = 0.722) and $R^2 = 0.521$ demonstrate that the corrected model explains more than half of the variability in the observed dataset. Meanwhile, the RMSE decrease from 179.66 mm/month to 131.42 mm/month indicates that MMBC has successfully adjusted systematic biases without altering the underlying temporal pattern of the model.

Table 2. Validation Metrics

Parameters	Uncorrected model	Corrected model
RMSE	179.664	131.421
Pearson Correlation (r)	0.323	0.722
Coefficient of Determination (R2)	0.105	0.521

3.2 Rainfall projection

The projected rainfall over Sumatera that was obtained from the bias-corrected CMIP6 EC-Earth3 dataset under the SSP5–8.5 scenario reveals interannual variability and a very fluctuating trend throughout the 21st century. Fig. 4 presents the spatially averaged annual precipitation for the period 2015–2100. Overall, the rainfall projection shows increased interannual variability, implying a more erratic rainfall pattern that suggests a possible intensification of dry years and the emergence of more frequent drought conditions. During the initial projection period, precipitation fluctuates markedly between approximately 1,800 and 4,000 mm per year; meanwhile, the 10-year moving average shows a relatively stable rainfall trend. This stability suggests that Sumatra's rainfall regime will persist within its historical range in the near term, in accordance with major ocean–atmosphere oscillation patterns such as the El Niño–Southern Oscillation (ENSO) and the Indian Ocean Dipole (IOD). Similar results were reported by Misnawati et al. (2023), who found that rainfall changes are projected to be insignificant compared to historical data in the near future.

Natural rainfall variability is likely to remain dominated by ocean-atmosphere oscillations patterns rather than anthropogenic factors during the early 21st century (Le & Bae, 2019).

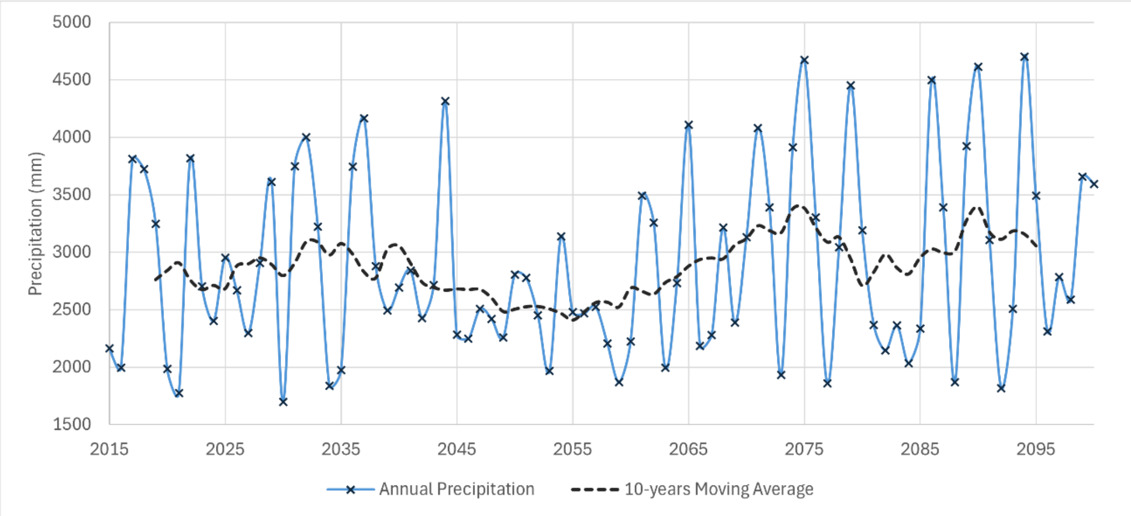

Fig. 4. Projected Annual Total Precipitation during 2015-2100 in Sumatra based on SSP5–8.5

Between 2036 and 2055, a moderate decline in rainfall is observed, with several dry anomalies in the mid-century period, with the moving average line decreasing to around 2,500 mm per year. This trend coincides with the projected intensification of warming and a shift in the regional circulation system, which may reduce convective activity over the western Maritime Continent (Steffen et al., 2023). The mid-century dry anomalies could correspond to more frequent or prolonged El Niño events, which have historically caused significant rainfall deficits in Sumatra (Suhadi et al., 2023).

Rainfall trends rose back during 2055–2075, indicated by the upward movement of the moving average from 2,500 to 3,400 mm/year. This period shows a partial recovery in precipitation totals and several wet anomalies where annual rainfall exceeds 4,000 mm. However, the moving average once again shows a slight gradual downward turn before fluctuating around 3,000 mm/year toward the end of the century, accompanied by much stronger interannual fluctuations compared to the early and mid-century periods. The amplitude of these variations becomes considerably larger, with extreme wet years exceeding 4,500 mm and dry years dropping close to 2,000 mm. This widening range of rainfall variability suggests that Sumatra's future hydroclimate will be characterized by more frequent and more severe extremes rather than steady drying periods (Nurlatifah et al., 2024). Consequently, when droughts occur, they are likely to be more intense and prolonged due to deeper rainfall deficits, while wet anomalies may bring heavier rainfall events.

3.3 Standardized precipitation index

The projected three-month Standardized Precipitation Index (SPI-3) for the period 2015–2100, derived from the bias-corrected CMIP6 EC-Earth3 dataset under the SSP5–8.5 scenario, illustrates pronounced temporal variability and an increasing frequency of drought events toward the end of the 21st century (Fig. 5). The SPI-3 time series provides a standardized representation of rainfall anomalies, where negative values indicate dry periods and positive values reflect wet conditions. Figure 6 shows that the SPI-3 fluctuates sharply throughout the projection period and shows an alternating wet and dry conditions at irregular intervals. The high frequency of oscillations around the zero line is similar with the fluctuating trends of rainfall patterns, marked by strong interannual variability as a results from the influence of ENSO and IOD (Suhadi et al., 2023).

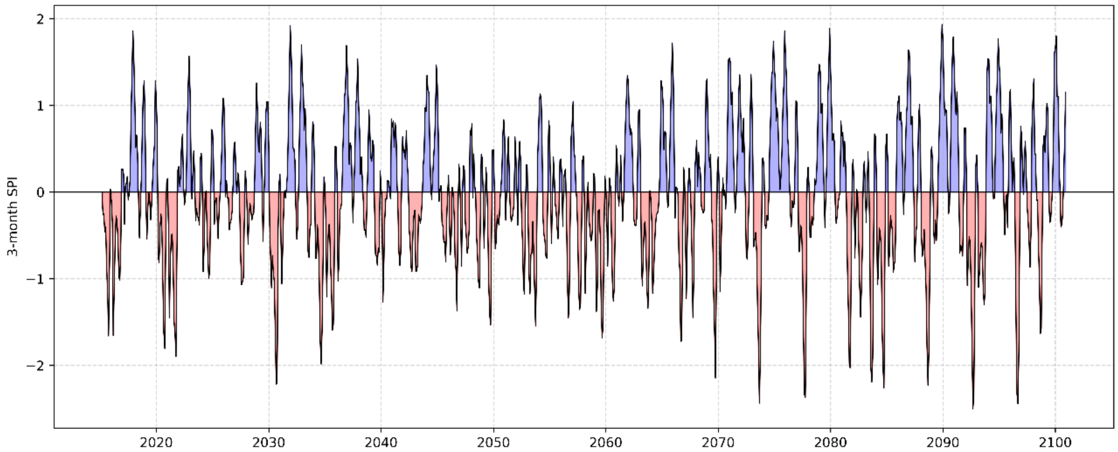

Fig. 5. Projected SPI-3 during 2015-2100 in Sumatra based on SSP5–8.5

During the early to mid-century projection period (2015–2065), SPI-3 values oscillate moderately between +1.5 and −1.5 that implies a balance between wet and dry events. However, the late-century portions (2065–2100) display more frequent and deeper excursions into negative territory, with several episodes falling below −1.5, classified as severe to extreme droughts according to BMKG classification. This finding aligns with Sara et al. (2024), who projected the onset of intensified drought conditions from mid-century onward under CMIP6 SSP scenarios, with the late-century period characterized by more severe and longer dry events across tropical regions. The pattern of recurrent negative SPI values observed in this study is consistent with other regional and global analyses. For instance, Song and Chung (2025) found that extreme drought events become more frequent and persistent toward the century's end across global land areas under SSP5–8.5. Similarly, Leerach et al. (2025) reported that future droughts in northern Thailand will occur more frequently but with shorter recovery intervals, indicating enhanced drought persistence under a warmer climate. Despite this tendency, the large interannual variability indicates substantial projection uncertainty.

Although SPI is a standardized metric with a mean of zero, the temporal evolution of the index suggests an asymmetric distribution of extremes, with negative anomalies becoming more prevalent than positive ones toward the latter half of the projection period (Bhardwaj et al., 2025). This imbalance implies a gradual shift toward a drier baseline climate, even though wet anomalies continue to occur sporadically. The persistence of wet spikes (SPI > +1.0) in several decades, such as around 2020–2035 and 2080–2090, highlights that future rainfall is not uniformly declining but will manifest in short, intense wet events separated by prolonged dry intervals (Hasegawa et al., 2016). Such an alternation between intense wet and prolonged dry periods is characteristic of hydroclimatic intensification, a phenomenon frequently reported in recent global climate model analyses (Zhao & Dai, 2021). Studies by Nguyen-Ngoc-Bich et al. (2022) and Phan-Van et al. (2022) demonstrated that under SSP5–8.5, the Indonesian region is expected to experience higher interannual rainfall variability, leading to a paradoxical pattern of more intense rainfall extremes yet longer dry spells. The SPI-3 series in Figure 6 reflects this dynamic, where increased oscillation amplitude indicates that both extremes — droughts and wet surges — may intensify simultaneously.

The persistence of negative SPI-3 values over multiple months suggests that droughts will become more frequent and intense as the century progresses (Su et al., 2021). This amplification of drought frequency corresponds with the observed decline in projected rainfall discussed in the previous section. Reduced mean precipitation and heightened variability together lead to more frequent subnormal rainfall conditions, which are reflected as consecutive negative SPI-3 values (Liu et al., 2024). Significant extreme dry events are noticeable at irregular intervals around 2060, 2078, 2084, and 2092. Such high-severity drought episodes will be a feature of the late-century hydroclimate under a high-emission trajectory (Cook et al., 2020). The magnitude and duration of projected SPI-3 droughts in this study are similar to those recorded during past El Niño years, such as 2015–2016, when Sumatra experienced one of its most severe droughts in recent history (Phan-Van et al., 2022). The SPI-3 projection underscores an emerging pattern of more frequent and prolonged meteorological droughts especially in the latter half of the century.

3.4 Drought identification

The identification of drought frequency across Sumatra from 2015 to 2100, based on the 3-month Standardized Precipitation Index (SPI3), provides a comprehensive view of the temporal and spatial variability of meteorological drought under the SSP5-8.5 climate scenario. Figure 7 presents the annual frequency of drought occurrences (SPI < –1.5) aggregated from all grid points across the island, while Figure 8 illustrates the spatial distribution of drought frequency during the projection period. Together, these visualizations allow for the interpretation of how droughts are likely to evolve over time and space in response to future climate conditions.

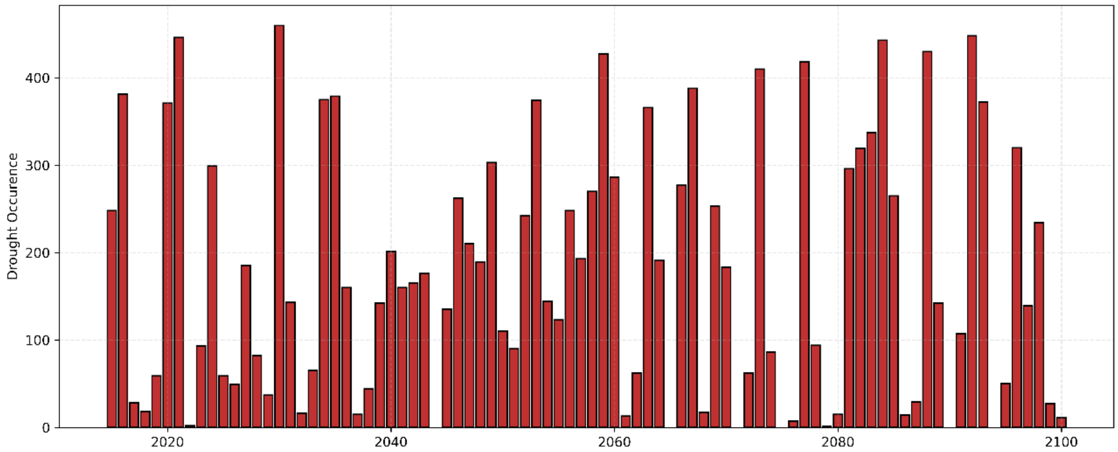

Fig. 6. Projected Annual Drought Occurence during 2015-2100 in Sumatra based on SSP5–8.5

As shown in Fig. 6, the frequency of drought events in Sumatra demonstrates strong interannual variability with noticeable multi-decadal fluctuations throughout the simulation period. Several peaks of extreme drought frequency are observed, particularly around the years 2020, 2030, 2060, and 2085, when the total number of grid cells experiencing severe droughts exceeds 400. These peaks indicate years dominated by widespread dryness across large parts of the island. In contrast, there are years with very few drought occurrences which suggest alternating cycles of dry and wet conditions. During the early decades of the projection, drought events appear more sporadic yet relatively intense, corresponding to transitional climate patterns under the near-future warming scenario. The mid-century period exhibits more frequent drought occurrences that consistent with the expected intensification of hydrometeorological extremes under higher global mean temperatures (Zhai et al., 2020). In this interval, several consecutive years show clustered drought frequencies, suggesting that the persistence of below-normal rainfall could extend over multiple seasons. Toward the end of the century, the pattern remains highly variable but tends to feature intense dry sequences which aligns with the anticipated amplification of interannual rainfall variability in tropical regions under high-emission scenarios (Song & Chung, 2024).

These projected fluctuations are comparable to the findings of previous studies. Zhao et al. (2023) reported that multi-decadal fluctuations in drought frequency are a common response to anthropogenic forcing superimposed on natural climate variability in the Indo-Pacific region. Similarly, Arango et al. (2021) found that drought frequency and duration in Southeast Asia are modulated by interannual to decadal variability associated with ENSO and the Pacific Decadal Oscillation. The pattern observed in Figure 7 thus suggests that Sumatra's hydroclimatic regime will likely experience greater temporal variability with alternating extremes of wet and dry years becoming more pronounced in the second half of the century. The overall number of drought events does not follow a simple linear trend. Instead, the variability indicates complex interactions between anthropogenic forcing and natural oscillations. The persistence of drought episodes clustered within certain decades implies the potential influence of multi-decadal climate modes such as the Pacific Decadal Oscillation (PDO) or long-term ENSO cycles (Zhu & Yang, 2020). These modes may modulate the effects of greenhouse-gas-driven warming on precipitation anomalies across the Indonesian maritime continent, leading to temporal irregularities in drought frequency.

3.5 Spatiotemporal drought characteristics

The spatial pattern of drought frequency shown in Figure 9 highlights clear regional disparities across Sumatra. The southern part of the island, particularly areas between 2°S and 6°S such as Lampung, South Sumatra, and parts of Bengkulu, exhibits the highest drought frequencies, exceeding 140 events during the projection period. These southern regions are strongly influenced by the Australian monsoon which results in a distinct and prolonged dry season each year. Furthermore, extensive land use for agriculture and plantations, such as oil palm and rubber, may exacerbate local dryness by altering evapotranspiration and soil moisture dynamics (Merten et al., 2020).

Center Sumatra, particularly the southern North Sumatra, Riau, and West Sumatera, shows comparatively fewer drought occurrences. This region lies within the equatorial rainfall zone influenced by the Intertropical Convergence Zone (ITCZ) which brings more frequent rainfall and mitigates drought occurrences (Jung et al., 2023). Meanwhile, northern Sumatra is characterized by an equatorial climate with a bimodal rainfall pattern, featuring two wet seasons and two relatively short dry seasons each year. Although the dry periods are generally brief, droughts can still occur when both dry seasons intensify during years influenced by large-scale climate anomalies such as El Niño (Qian, 2020).

This spatial differentiation is also consistent with earlier drought assessments in Indonesia. A study by Hadiningrum et al. (2023) across the Indonesian archipelago found that southern Sumatra and Java are among the most drought-prone regions under future scenarios due to stronger seasonal rainfall concentration and a higher sensitivity to El Niño events. Similarly, Liu et al. (2020) reported that the southern part of Sumatra tends to experience greater interannual rainfall variability, which increases the likelihood of prolonged dry episodes. The present findings reinforce those conclusions, providing quantitative evidence that southern Sumatra will remain a critical hotspot for drought risk through the end of the 21st century.

The integrated temporal–spatial assessment reveals that future drought regimes in Sumatra are projected to exhibit increased frequency and wider spatial coverage of severe droughts, particularly during the mid- and late 21st century. This intensification of meteorological stress is consistent with regional trends across Southeast Asia under SSP5-8.5, where enhanced land–sea thermal contrasts delay monsoon onset and shorten wet seasons, leading to reduced soil moisture and groundwater recharge (Yahaya et al., 2024). Southern Sumatra, in particular, is expected to face more persistent droughts linked to elevated evapotranspiration and declining precipitation, exacerbating hydrological and agricultural stress (Su et al., 2021). The clustering of extreme SPI3 drought years indicates intensified interannual variability which is similar to projections in Thailand and Vietnam that suggest a 30–50% rise in drought frequency after 2050 (Leerach et al., 2025; Nguyen-Xuan et al., 2025). The coherence of projected SPI trends across Sumatra, Java, and Kalimantan supports the interpretation that drought intensification reflects broader Indo-Pacific climatic responses to anthropogenic forcing rather than localized anomalies (Zeng et al., 2022; Bhardwaj et al., 2025).

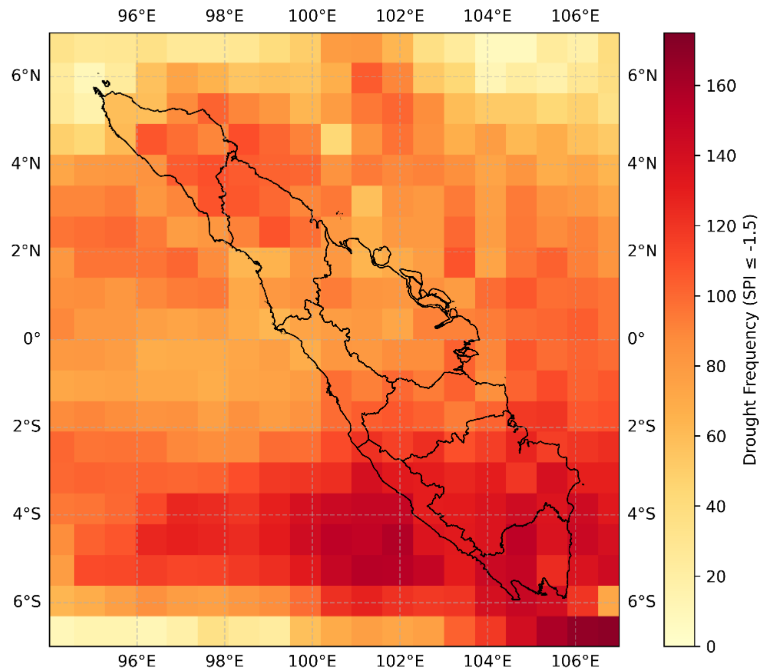

Fig. 7. Projected Annual Drought Frequency during 2015-2100 in Sumatra based on SSP5–8.5

The seasonal analysis of drought frequency across Sumatra based on the 3-month Standardized Precipitation Index (SPI3) provides deeper insights into the temporal distribution of dryness throughout the year and its spatial variations under the SSP5–8.5 scenario. Figure 8 to Figure 11 illustrates the spatial distribution of drought frequency (SPI < −1.5) for each climatological season: December–January–February (DJF), March–April–May (MAM), June–July–August (JJA), and September–October–November (SON). These maps reveal clear differences in both intensity and geographical extent of drought across the four seasonal periods, reflecting the strong influence of monsoonal transitions and intertropical convergence dynamics on rainfall patterns in the region.

During the DJF season, Sumatra experiences the lowest frequency of severe droughts (SPI ≤ −1.5) across the annual cycle, with all regions registering fewer than 40 events over the 85 years projection period (Fig. 8). This distribution suggests that the austral summer remains as the wettest phase for most of the island, supported by the active northwest monsoon that transports abundant moisture from the Indian Ocean. Even southern regions, such as Lampung and South Sumatra retain sufficient rainfall to prevent widespread drought. This relatively uniform moisture availability reflects the southward position of the ITCZ and strong monsoonal convection which allows DJF to function as a hydrological recharge period for soil and groundwater systems (Ramotubei et al., 2025). In contrast, drought frequency increases in northern Sumatra during MAM, particularly particularly across Aceh, North Sumatra, and northern Riau, where SPI ≤ −1.5 events exceed 120 occurrences. These regions experiences the transition between the wet northwest monsoon to the early dry southeast monsoon, which produces temporary rainfall deficits characteristic of the equatorial bimodal rainfall regime (Ferijal et al., 2025). Under SSP5–8.5, this seasonal shift suggests an earlier onset of dry conditions and enhanced interannual rainfall variability linked to ENSO–IOD–ITCZ interactions (Mamani et al., 2025).

The JJA period marks a transitional phase before the onset of the primary dry season with most regions register fewer than 60 drought events (SPI ≤ −1.5), indicating that widespread dryness has not yet developed. This pattern is consistent with broader Indo-Pacific climate behavior, where the gradual displacement of the ITCZ and cross-equatorial flow delays the full establishment of the dry southeast monsoon (Lee et al., 2022). Nevertheless, this period acts as a precursor to the primary dry season by gradually reducing moisture storage under rising temperatures and evapotranspiration, thereby increasing vulnerability to subsequent drought intensification (Muthuvel & Qin, 2025). The peak of drought occurrence emerges during SON, particularly across southern Sumatra, where persistent dry continental air masses and suppressed convection delay the onset of the wet season and produce over 120 drought events in Lampung, South Sumatra, and southern Jambi. These conditions correspond to the late phase of the southeast monsoon and are often associated with enhanced subsidence and limited rainfall recovery (Gebregiorgis et al., 2019). These processes explain why SON remains a climatological drought maximum in the southern equatorial belt, contrasting sharply with the earlier wet onset observed in northern Sumatra. The SON period also coincides with Indonesia's peak fire period, which creates land–atmosphere feedbacks that amplify dryness during late monsoon transitions (Ullah et al., 2022). Under continued warming, CMIP6 projections indicate that intensified atmospheric drying may prolong this fire-prone window and reinforce drought persistence in southern Sumatra (Huang et al., 2022).

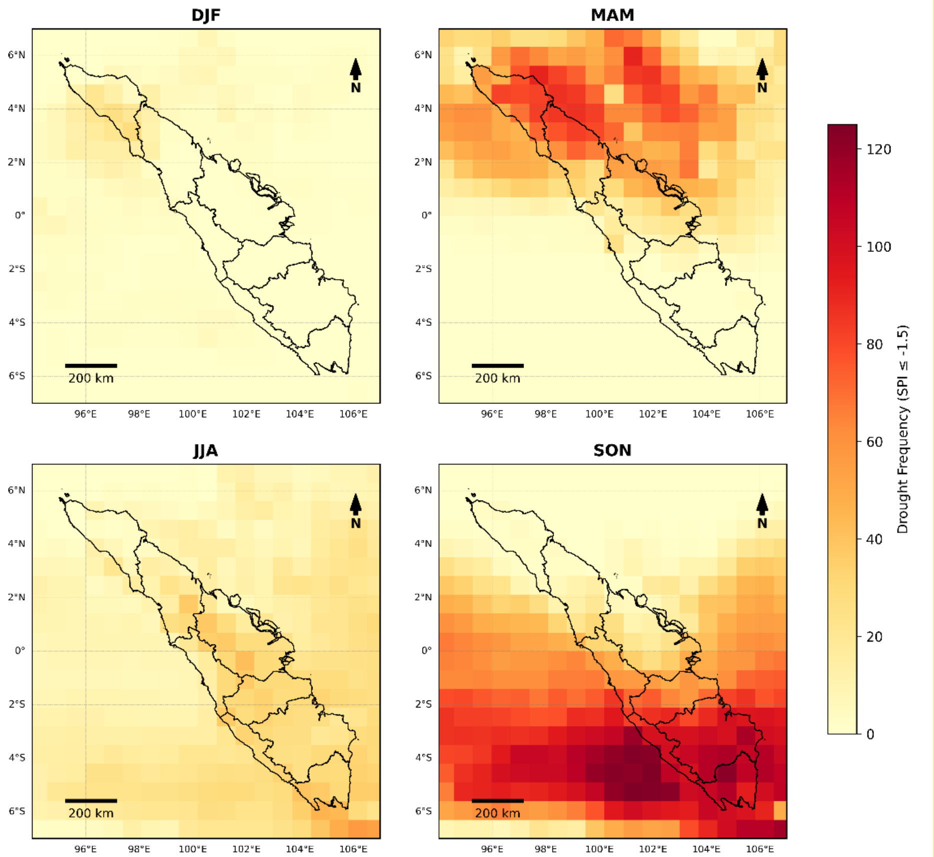

Fig. 8. Projected Seasonal Drought Frequency during 2015-2100 in Sumatra based on SSP5–8.5

The four seasonal drought maps collectively delineate a coherent hydroclimatic rhythm over Sumatra where drought intensity and spatial extent oscillate latitudinally throughout the year in response to large-scale atmospheric circulation. Droughts prevail across southern Sumatra during DJF and SON, reflecting the suppressed convection associated with the southward displacement of the ITCZ and the dominance of the southeast monsoon's dry continental flow. Conversely, MAM marks a northward concentration of drought linked to the first dry phase of the equatorial rainfall regime, while JJA remains comparatively moist due to residual convective activity and transitional moisture transport. These shifts correspond closely to the annual ITCZ migration and its modulation by coupled ocean–atmosphere modes, particularly ENSO and the Indian Ocean Dipole (IOD), which jointly govern convection and rainfall over the Indonesian maritime continent (Ramotubei et al., 2025).

The spatial coherence of these seasonal transitions highlights the integrated influence of tropical teleconnections, land–sea thermal contrast, and topographic modulation on drought distribution. CMIP6-based assessments indicate that anthropogenic warming enhances the amplitude of ITCZ shifts and the persistence of dry anomalies, particularly in southern Sumatra where fire-prone peatlands coincide with recurrent drought peaks (Gillett et al., 2022). Furthermore, the future intensification of SON droughts under SSP5–8.5 reflects a delayed monsoon onset consistent with altered Indo-Pacific teleconnection pathways (Fan & Meng, 2023). The projected increase in SPI ≤ −1.5 events, even during typically wet seasons, signals a shift toward a more variable and arid hydroclimate regime. Such transformations imply that Sumatra's hydrological future will be characterized not only by mean drying but also by enhanced seasonal irregularity, necessitating adaptive land-use and water-management strategies to mitigate compounding risks of drought, fire, and reduced agricultural productivity (Ty et al., 2022).

The projected seasonal variations in drought frequency have direct implications for agriculture, water resource management, and fire mitigation strategies. The DJF and SON seasons, which show the highest drought concentrations in southern Sumatra, are likely to experience the most severe hydrological stress and associated socio-economic impacts. Conversely, MAM droughts in the north could disrupt agricultural calendars and threaten the stability of water supply systems that rely on early wet-season inflows. Adaptation strategies should therefore be seasonally and regionally differentiated. In southern Sumatra, water storage and irrigation systems must be strengthened to buffer the dual DJF–SON drought peaks. In northern regions, early-season drought preparedness and diversification of crop calendars could help mitigate MAM-related rainfall deficits. Moreover, since JJA represents a relatively quiescent period in terms of drought frequency, it could serve as an optimal window for water resource recovery and storage.

The findings of this study should be interpreted in light of several methodological considerations. The analysis employs a single CMIP6 model to focus on the SSP5–8.5 high-emission pathway to emphasize potential drought responses under sustained warming climate. In addition, the SPI metric is based solely on precipitation and therefore reflects meteorological drought conditions without explicitly accounting for evapotranspiration or land-surface feedbacks. The model's spatial resolution (~100 km) may also limit the representation of localized topographic influences such as those associated with the Barisan Mountain range. Nevertheless, this scale remains appropriate for capturing broader regional hydroclimatic patterns that are central to the objectives of this study.

4. Conclusions

Drought projections for Sumatra through 2100 under the high-emission SSP 5-8.5 scenario indicate a fundamental shift toward a more unstable and extreme hydroclimatic regime. A primary finding of this study is the synthesis that the frequency and intensity of meteorological droughts (SPI < -1.5) will increase, particularly in the latter half of the century. Instead of a simple linear shift toward drier conditions, the projections reveal a pattern of hydroclimatic intensification, where severe yet relatively short drought periods will occur more frequently, interspersed with extreme wet events. This sharp increase in interannual variability, driven by the amplification of large-scale atmospheric circulations like ENSO and the IOD by anthropogenic pressures, presents significant challenges to predictability and water resource management.

Spatially, this study quantitatively identifies the southern part of Sumatra—encompassing provinces like Lampung and South Sumatra—as the most vulnerable regional hotspot, with a projection of over 140 severe drought events. More importantly, an original finding of this study is the mapping of a clear seasonal duality in drought vulnerability. The northern region, which has an equatorial rainfall pattern, exhibits peak vulnerability during the March-May (MAM) period. Conversely, the monsoon-influenced southern region experiences its peak drought during September-November (SON), coinciding with the region's peak fire season. By integrating bias-corrected CMIP6 projections with robust SPI calculations, this study provides a scientific contribution in the form of a new, comprehensive, and spatiotemporally detailed understanding of future drought risk. This synthesis surpasses previous historical analyses and offers key insights crucial for developing climate adaptation strategies and sustainable water management. These findings underscore the need of a non-one-size-fits-all approach for mitigation strategies that specifically tailored to the unique regional hotspots and seasonal vulnerabilities within Sumatra.

Acknowledgement

The author would like to express their sincere gratitude to all those who supported and contributed to the success of this research.

Author Contribution

Conceptualization, A. N.; Methodology, A. N.; Software, A. N.; Validation, A. N.; Formal Analysis, A. N.; Investigation, A. N.; Resources, A. N.; Data Curation, A. N.; Writing—Original Draft Preparation, A. N.; Writing—Review & Editing, A. N.; Visualization, A. N.; Supervision, A. N.; Proje ct Administration, A. N.; Funding Acquisition, A. N.

Funding

This research received no external funding.

Ethical Review Board Statement

Not available.

Informed Consent Statement

Not available.

Data Availability Statement

The CMIP6 EC-Earth3 model precipitation data analyzed in this study are publicly available from the Copernicus Climate Change Service (C3S) Climate Data Store at [https://cds.climate.copernicus.eu/datasets/projections-cmip6]. The observational rainfall data from BMKG stations were obtained from the Indonesian Agency for Meteorology, Climatology, and Geophysics (BMKG) and may be available upon request, subject to the agency's data sharing policies. The derived datasets generated during the current study, such as the bias-corrected precipitation values and Standardized Precipitation Index (SPI) results, are available from the corresponding author upon reasonable request.

Conflicts of Interest

The author declares no conflict of interest.

Declaration of Generative AI Use

During the preparation of this work, the author used a generative AI tool to assist in improving the grammar, clarity, and academic tone of the manuscript. After using this tool, the author reviewed and edited the content as needed and took full responsibility for the content of the publication.

Open Access

References

Akhsan, H., Irfan, M., Supari, S., & Iskandar, I. (2023). Dynamics of extreme rainfall and its impact on forest and land fires in the eastern coast of Sumatra. *Science & Technology Indonesia*, *8*(3), 403–413. https://doi.org/10.26554/sti.2023.8.3.403-413

Arango, J. D. P., Lintner, B. R., Carvalho, L. M. V., & Lyon, B. (2021). Spatial extents of tropical droughts during El Niño in current and future climate in observations, reanalysis, and CMIP5 models. *Geophysical Research Letters*, *48*(14). https://doi.org/10.1029/2021gl093701

Batibeniz, F., Hauser, M., & Seneviratne, S. I. (2023). Countries most exposed to individual and concurrent extremes and near-permanent extreme conditions at different global warming levels. *Earth System Dynamics*, *14*(2), 485–505. https://doi.org/10.5194/esd-14-485-2023

Bhardwaj, K., Mishra, A., & Khedun, C. P. (2025). Global droughts in a warming climate: Evaluation of SPI and SPEI under 1.5 , 2 , and 3 C global warming. *Journal of Hydrology*, 133309. https://doi.org/10.1016/j.jhydrol.2025.133309

Cammalleri, C., McCormick, N., Spinoni, J., & Nielsen-Gammon, J. W. (2024). An Analysis of the Lagged Relationship between Anomalies of Precipitation and Soil Moisture and Its Potential Role in Agricultural Drought Early Warning. *Journal of Applied Meteorology and Climatology*, *63*(2), 339–350. https://doi.org/10.1175/jamc-d-23-0077.1

Cook, B. I., Mankin, J. S., Marvel, K., Williams, A. P., Smerdon, J. E., & Anchukaitis, K. J. (2020). Twenty-First century drought projections in the CMIP6 forcing scenarios. *Earth S Future*, *8*(6). https://doi.org/10.1029/2019ef001461

Copernicus Climate Change Service. (2021). CMIP6 climate projections [Dataset]. In *Climate Data Store (CDS)*.

Daliakopoulos, I. N. (2021). Precipitation mapping and spatial analysis using R. In *Elsevier eBooks* (pp. 173–192). https://doi.org/10.1016/b978-0-12-822699-5.00008-2

Ernst, J., Stojanovic, M., & Sorí, R. (2025). Historical and Future Drought Intensification in the Pantanal Wetland: Evidence from Multi-Source Weather Data and CMIP6 Multi-Model Projections. Environments, 12(11), 413. https://doi.org/10.3390/environments12110413

Fan, L., & Meng, X. (2023). The Asymmetric Predictive Power of Indian Ocean Dipole for subsequent year's ENSO: Role of Atlantic Ocean as an Intermediary. *Geophysical Research Letters*, *50*(22). https://doi.org/10.1029/2023gl105525

Fathiyana, R. Z., Haryadi, D., Ananda, N., Hidayat, D. J., Wicaksana, H. S., Azahra, R. W., & Saputra, H. G. (2025). Application of neural networks for drought forecasting based on the standardised precipitation index. *Journal of Water and Land Development*, 113–121. https://doi.org/10.24425/jwld.2025.154255

Fattorini, L., Franceschi, S., Marcheselli, M., Pisani, C., & Pratelli, L. (2023). Design-based spatial interpolation with data driven selection of the smoothing parameter. *Environmental and Ecological Statistics*, *30*(1), 103–129. https://doi.org/10.1007/s10651-023-00555-w

Ferijal, T., Mechram, S., & Fauzi, A. (2025). Spatial and temporal analysis of dry spell variability in Aceh, Indonesia: Implications for drought mitigation and agricultural planning. *IOP Conference Series Earth and Environmental Science*, *1476*(1), 012009. https://doi.org/10.1088/1755-1315/1476/1/012009

Gao, H., Jing, J., & Dou, S. (2024). Factor-driven impact analysis based on the Standardized Precipitation Index. In *Proceedings of SPIE - The International Society for Optical Engineering*. SPIE. https://doi.org/10.1117/12.3035590

Gebregiorgis, D., Rayner, D., & Linderholm, H. W. (2019). Does the IOD independently influence seasonal monsoon patterns in northern Ethiopia? *Atmosphere*, *10*(8), 432. https://doi.org/10.3390/atmos10080432

Gillett, Z. E., Hendon, H. H., Arblaster, J. M., Lin, H., & Fuchs, D. (2022). On the Dynamics of Indian Ocean Teleconnections into the Southern Hemisphere during Austral Winter. *Journal of the Atmospheric Sciences*, *79*(9), 2453–2469. https://doi.org/10.1175/jas-d-21-0206.1

Hadiningrum, T., Lestari, D. O., & Trismidianto, N. (2023). Comparison influencing of El-Nino Southern oscillation and Indian Ocean dipole on rainfall variability during the Asian winter and summer monsoon over Indonesian maritime continent. In *Springer proceedings in physics* (pp. 291–302). https://doi.org/10.1007/978-981-19-9768-6_28

Hasegawa, A., Gusyev, M., & Iwami, Y. (2016). Meteorological drought and flood assessment using the Comparative SPI approach in Asia under climate change. *Journal of Disaster Research*, *11*(6), 1082–1090. https://doi.org/10.20965/jdr.2016.p1082

He, C., Liu, Z., Wu, J., Pan, X., Fang, Z., Li, J., & Bryan, B. A. (2021). Future global urban water scarcity and potential solutions. *Nature Communications*, *12*(1). https://doi.org/10.1038/s41467-021-25026-3

Hendrawan, V. S. A., Mawandha, H. G., Sakti, A. D., Karlina, N., Andika, N., Shahid, S., & Jayadi, R. (2024). Future exposure of rainfall and temperature extremes to the most populous island of Indonesia: A projection based on CORDEX simulation. *International Journal of Climatology*, *44*(10), 3529–3547. https://doi.org/10.1002/joc.8537

Hu, C., Lian, T., Cheung, H., Qiao, S., Li, Z., Deng, K., Yang, S., & Chen, D. (2020). Mixed diversity of shifting IOD and El Niño dominates the location of Maritime Continent autumn drought. *National Science Review*, *7*(7), 1150–1153. https://doi.org/10.1093/nsr/nwaa020

IPCC. (2023). *Climate Change 2021 – The Physical Science Basis: Working Group I Contribution to the Sixth Assessment Report of the Intergovernmental Panel on Climate Change*. Cambridge University Press. https://doi.org/10.1017/9781009157896

Irwandi, H., Rosid, M. S., & Mart, T. (2021). The effects of ENSO, climate change and human activities on the water level of Lake Toba, Indonesia: a critical literature review. *Geoscience Letters*, *8*(1). https://doi.org/10.1186/s40562-021-00191-x

Jo, K., & Pak, K. (2022). Demonstrating the bias-correction impact on regional climate model (RegCM) over the Democratic People's Republic of Korea: Implication for temperature and precipitation. *Journal of Earth System Science*, *131*(2). https://doi.org/10.1007/s12040-022-01836-x

Johny, K., Pai, M. L., & Adarsh, S. (2020). An investigation on drought teleconnection with indian ocean dipole and el-nino southern oscillation for peninsular india using time dependent intrinsic correlation. *IOP Conference Series Earth and Environmental Science*, *491*(1), 012007. https://doi.org/10.1088/1755-1315/491/1/012007

Jung, H., Knippertz, P., Ruckstuhl, Y., Redl, R., Janjic, T., & Hoose, C. (2023). Understanding the dependence of mean precipitation on convective treatment and horizontal resolution in tropical aquachannel experiments. *Weather and Climate Dynamics*, *4*(4), 1111–1134. https://doi.org/10.5194/wcd-4-1111-2023

Kurniadi, A., Weller, E., Kim, Y., & Min, S. (2022). Evaluation of Coupled Model Intercomparison Project Phase 6 model-simulated extreme precipitation over Indonesia. *International Journal of Climatology*, *43*(1), 174–196. https://doi.org/10.1002/joc.7744

Le, T., & Bae, D. (2019). Causal links on interannual timescale between ENSO and the IOD in CMIP5 future simulations. *Geophysical Research Letters*, *46*(5), 2820–2828. https://doi.org/10.1029/2018gl081633

Lee, J., Kang, S. M., Kim, H., & Xiang, B. (2022). Disentangling the effect of regional SST bias on the double-ITCZ problem. *Climate Dynamics*, *58*(11–12), 3441–3453. https://doi.org/10.1007/s00382-021-06107-x

Leerach, K., Iamchuen, N., Thanawong, K., Busababodhin, P., Kirtsaeng, S., & Pimonsree, S. (2025). Meso-scale spatiotemporal analysis of future drought characteristics in Northern Thailand under climate change and variability. *Theoretical and Applied Climatology*, *156*(8). https://doi.org/10.1007/s00704-025-05662-1

Li, Y., Yan, D., Peng, H., & Xiao, S. (2020). Evaluation of precipitation in CMIP6 over the Yangtze River Basin. *Atmospheric Research*, *253*, 105406. https://doi.org/10.1016/j.atmosres.2020.105406

Liu, S., Raghavan, S. V., Ona, B. J., & Nguyen, N. S. (2023). Bias evaluation in rainfall over Southeast Asia in CMIP6 models. *Journal of Hydrology*, *621*, 129593. https://doi.org/10.1016/j.jhydrol.2023.129593

Liu, S., Zhang, H., Shi, X., Chen, M., Cao, P., Li, Z., Troa, R. A., Zuraida, R., Triarso, E., & Marfasran, H. (2020). Reconstruction of monsoon evolution in southernmost Sumatra over the past 35 kyr and its response to northern hemisphere climate changes. *Progress in Earth and Planetary Science*, *7*(1). https://doi.org/10.1186/s40645-020-00349-9

Liu, Y., Chen, X., Bai, Y., & Zeng, J. (2024). Evaluation of 22 CMIP6 model-derived global soil moisture products of different shared socioeconomic pathways. *Journal of Hydrology*, *636*, 131241. https://doi.org/10.1016/j.jhydrol.2024.131241

Mahadevan, M., Noel, J. K., Umesh, M., Santhosh, A. S., & Suresh, S. (2024). Climate Change Impact on Water Resources, Food Production and Agricultural Practices. In *The Climate–Health– Sustainability Nexus* (pp. 207–229). https://doi.org/10.1007/978-3-031-56564-9_9

Mamani, L., Andreoli, R. V., De Souza, I. P., Cevalho, W., Sales, D., Kayano, M. T., De Souza, R. a. F., Molina-Carpio, J., Ceron, W. L., & Macedo, T. (2025). Extreme droughts in the Amazon Basin during cyclic ENSO events coupled with Indian Ocean Dipole modes and Tropical North Atlantic warming. *The Science of the Total Environment*, *963*, 178536. https://doi.org/10.1016/j.scitotenv.2025.178536

Mareta, L., Agiel, H., & Hadiningrum, T. (2024). Historical and projected rainfall climatology in Sumatra based on the CMIP6. *IOP Conference Series Earth and Environmental Science*, *1359*(1), 012089. https://doi.org/10.1088/1755-1315/1359/1/012089

McKee, T. B., Doesken, N. J., & Kleist, J. (1993). The relationship of drought frequency and duration to time scale. *Proceedings of the Eighth Conference on Applied Climatology*, 179–184. http://clima1.cptec.inpe.br/~rclima1/pdf/paper_spi.pdf

Merten, J., Stiegler, C., Hennings, N., Purnama, E. S., Röll, A., Agusta, H., Dippold, M. A., Fehrmann, L., Gunawan, D., Hölscher, D., Knohl, A., Kückes, J., Otten, F., Zemp, D. C., & Faust, H. (2020). Flooding and land use change in Jambi Province, Sumatra: integrating local knowledge and scientific inquiry. *Ecology and Society*, *25*(3). https://doi.org/10.5751/es-11678-250314

Mukasa, J., Olaka, L., & Said, M. Y. (2020). Drought and households' adaptive capacity to water scarcity in Kasali, Uganda. *Journal of Water and Climate Change*, *11*(S1), 217–232. https://doi.org/10.2166/wcc.2020.012

Muthuvel, D., & Qin, X. (2025). Probabilistic analysis of future drought propagation, persistence, and spatial concurrence in monsoon-dominant Asian regions under climate change. *Hydrology and Earth System Sciences*, *29*(14), 3203–3225. https://doi.org/10.5194/hess-29-3203-2025

Nguyen-Ngoc-bich, P., Phan-Van, T., Trinh-Tuan, L., Tangang, F. T., Cruz, F., Santisirisomboon, J., Juneng, L., Chung, J. X., & Aldrian, E. (2022). Projected future changes in drought characteristics over Southeast Asia. *Vietnam Journal of Earth Sciences*, *44*(1), 127–144. https://doi.org/10.15625/2615-9783/16974

Nguyen-Xuan, T., Nguyen-Le, D., Tran-Anh, Q., Nguyen-Duy, T., & Ngo-Duc, T. (2025). Assessment of future droughts in Vietnam using high-resolution downscaled CMIP6 projections. *Natural Hazards*. https://doi.org/10.1007/s11069-025-07651-z

Nurlatifah, A., Hatmaja, R. B., Adany, F., & Darojatun, A. (2024). Impact of climate change on extreme precipitation events over Sumatera Island and the Malay Peninsula. *International Journal of Global Warming*, *32*(4), 374–398. https://doi.org/10.1504/ijgw.2024.137168

O'Neill, B. C., Kriegler, E., Ebi, K. L., Kemp-Benedict, E., Riahi, K., Rothman, D. S., Van Ruijven, B. J., Van Vuuren, D. P., Birkmann, J., Kok, K., Levy, M., & Solecki, W. (2017). The roads ahead: Narratives for shared socioeconomic pathways describing world futures in the

21st century. *Global Environmental Change*, *42*, 169–180. https://doi.org/10.1016/j.gloenvcha.2015.01.004

Phan-Van, T., Nguyen-Ngoc-Bich, P., Ngo-Duc, T., Vu-Minh, T., Le, P. V. V., Trinh-Tuan, L., Nguyen-Thi, T., Pham-Thanh, H., & Tran-Quang, D. (2022). Drought over Southeast Asia and Its Association with Large-Scale Drivers. *Journal of Climate*, *35*(15), 4959–4978. https://doi.org/10.1175/jcli-d-21-0770.1

Qian, J. (2020). Multi-scale climate processes and rainfall variability in Sumatra and Malay Peninsula associated with ENSO in boreal fall and winter. *International Journal of Climatology*, *40*(9), 4171–4188. https://doi.org/10.1002/joc.6450

Ramotubei, T. S., Landman, W. A., Mateyisi, M. J., Nangombe, S., & Beraki, A. F. (2025). Response of the global ITCZ to different ENSO phases and how the ITCZ determined from the maximum precipitation compares with the surface tropical wind convergence. *Environmental Development*, 101210. https://doi.org/10.1016/j.envdev.2025.101210

Sara, M., Mohamed, S., Brahim, L., & Rachid, I. (2024). Projection of future drought characteristics in Morocco under CMIP6 Scenario SSP2-4.5. *Bulletin De L'Institut Scientifique, Section Sciences De La Terre*, *46*, 83–96.

Satiadi, D., Purwaningsih, A., Harjupa, W., Saufina, E., Fathrio, I., Trismidianto, N., Rahmatia, F., Pratama, R., Hashiguchi, H., & Shimomai, T. (2025). Study of orography–MJO interaction and its impact on rainfall variability in West Sumatra. *Journal of Earth System Science*, *134*(2). https://doi.org/10.1007/s12040-025-02565-7

Sayama, T., Araki, R., Yamamoto, K., & Apip, N. (2021). Characteristics of soil and hillslope responses in humid tropical forests in Sumatra, Indonesia. *Hydrological Research Letters*, *15*(2), 23–30. https://doi.org/10.3178/hrl.15.23

Singh, H. V., Joshi, N., & Suryavanshi, S. (2023). Projected climate extremes over agro-climatic zones of Ganga River Basin under 1.5, 2, and 3° global warming levels. *Environmental Monitoring and Assessment*, *195*(9). https://doi.org/10.1007/s10661-023-11663-2

Song, Y. H., & Chung, E. (2024). Uncertainties in Future Extreme Drought Characteristics Associated with SSP Scenarios over Global Lands. *Earth Systems and Environment*. https://doi.org/10.1007/s41748-024-00505-x

Steffen, J., Seo, H., Clayson, C. A., Pei, S., & Shinoda, T. (2023). Impacts of tidal mixing on diurnal and intraseasonal air-sea interactions in the Maritime Continent. *Deep Sea Research Part II Topical Studies in Oceanography*, *212*, 105343. https://doi.org/10.1016/j.dsr2.2023.105343

Su, B., Huang, J., Mondal, S. K., Zhai, J., Wang, Y., Wen, S., Gao, M., Lv, Y., Jiang, S., Jiang, T., & Li, A. (2020). Insight from CMIP6 SSP-RCP scenarios for future drought characteristics in China. *Atmospheric Research*, *250*, 105375. https://doi.org/10.1016/j.atmosres.2020.105375

Suhadi, S., Iskandar, I., Supari, S., Irfan, M., & Akhsan, H. (2023). Extreme drought assessment in Sumatra-Indonesia using SPI and EDI. *Science & Technology Indonesia*, *8*(4), 691–700. https://doi.org/10.26554/sti.2023.8.4.691-700

Suhana, L., Tan, M. L., Luhaim, Z., Ramli, M. H. P., Subki, N. S., Tangang, F., & Ishak, A. M. (2023). Spatiotemporal characteristics of hydro-meteorological droughts and their connections to large-scale atmospheric circulations in the Kelantan River Basin, Malaysia. *Water Science & Technology Water Supply*, *23*(6), 2283–2298. https://doi.org/10.2166/ws.2023.126

Tang, B., Hu, W., & Duan, A. (2021). Assessment of Extreme Precipitation Indices over Indochina and South China in CMIP6 Models. *Journal of Climate*, *34*(18), 7507–7524. https://doi.org/10.1175/jcli-d-20-0948.1

Tang, T., Ge, J., Shi, H., Wang, L., Cao, J., & Lee, X. (2025). Drought frequency, intensity, and exposure have increased due to historical land use and land cover changes. *Communications Earth & Environment*, *6*(1). https://doi.org/10.1038/s43247-025-02392-0

Tuel, A., Choi, Y., AlRukaibi, D., & Eltahir, E. a. B. (2021). Extreme storms in Southwest Asia (Northern Arabian Peninsula) under current and future climates. *Climate Dynamics*, *58*(5–6), 1509–1524. https://doi.org/10.1007/s00382-021-05975-7

Ukkola, A. M., De Kauwe, M. G., Roderick, M. L., Abramowitz, G., & Pitman, A. J. (2020). Robust future changes in meteorological drought in CMIP6 projections despite uncertainty in precipitation. *Geophysical Research Letters*, *47*(11). https://doi.org/10.1029/2020gl087820

Ullah, I., Ma, X., Asfaw, T. G., Yin, J., Iyakaremye, V., Saleem, F., Xing, Y., Azam, K., & Syed, S. (2022). Projected changes in increased drought risks over South Asia under a warmer climate. *Earth S Future*, *10*(10). https://doi.org/10.1029/2022ef002830

Van Ty, T., Lavane, K., Nguyen, P. C., Downes, N. K., Nam, N. D. G., Minh, H. V. T., & Kumar, P. (2022). Assessment of Relationship between Climate Change, Drought, and Land Use and Land Cover Changes in a Semi-Mountainous Area of the Vietnamese Mekong Delta. *Land*, *11*(12), 2175. https://doi.org/10.3390/land11122175

Wang, Q., Zhang, R., Qi, J., Zeng, J., Wu, J., Shui, W., Wu, X., & Li, J. (2022). An improved daily standardized precipitation index dataset for mainland China from 1961 to 2018. *Scientific Data*, *9*(1). https://doi.org/10.1038/s41597-022-01201-z

Zeng, J., Li, J., Lu, X., Wei, Z., Shangguan, W., Zhang, S., Dai, Y., & Zhang, S. (2022). Assessment of global meteorological, hydrological and agricultural drought under future warming based on CMIP6. *Atmospheric and Oceanic Science Letters*, *15*(1), 100143. https://doi.org/10.1016/j.aosl.2021.100143

Zhang, Y., & Li, Z. (2020). Uncertainty analysis of standardized precipitation index due to the effects of probability distributions and parameter errors. *Frontiers in Earth Science*, *8*. https://doi.org/10.3389/feart.2020.00076

Zhao, T., & Dai, A. (2021). CMIP6 model-projected Hydroclimatic and Drought Changes and their Causes in the 21st Century. *Journal of Climate*, 1–58. https://doi.org/10.1175/jcli-d-21-0442.1

Zhao, Y., Di Lorenzo, E., Newman, M., Capotondi, A., & Stevenson, S. (2023). A Pacific Tropical decadal variability challenge for climate models. *Geophysical Research Letters*, *50*(15). https://doi.org/10.1029/2023gl104037

Zhu, Y., & Yang, S. (2020). Interdecadal and interannual evolution characteristics of the global surface precipitation anomaly shown by CMIP5 and CMIP6 models. *International Journal of Climatology*, *41*(S1). https://doi.org/10.1002/joc.6756

Biography of Author

Asshaffa Naim, Department of Environmental Geography, Faculty of Geography, Universitas Gadjah Mada, Sleman, Special Region of Yogyakarta 55281, Indonesia.

- Email: asshaffa.naim@mail.ugm.ac.id
- ORCID: N/A
- Web of Science ResearcherID: N/A
- Scopus Author ID: N/A
- Homepage: N/A